FRINGE2023
University of Leeds, UK | 11 - 15 September 2023

Deep neural network based automatic grounding line delineation in DInSAR interferograms

Sindhu Ramanath Tarekere[1], Lukas Krieger[1], Konrad Heidler[2], Dana Floricioiu[1]
[1]Remote Sensing Technology Institute, German Aerospace Center, Wessling, Germany
[2]Data Science in Earth Observation, Technical University of Munich, Germany

Motivation

Grounding lines are subsurface geophysical features that represent the boundary between grounded ice and floating ice shelves. Here, ice shelves experience flexure due to tidal forcing, which results in a temporary displacement of the grounding line.

Differential Interferometric SAR (DInSAR) captures the vertical deformation that occurs at the grounding zone due to tidal forcing. The current approach of manually delineating the grounding line location (GLL) on DInSAR interferograms is unfeasible on a large scale and inconsistent due to the subjective interpretation of human operators.

We developed a workflow that utilizes a deep neural network to automatically delineate grounding lines in DInSAR interferograms.

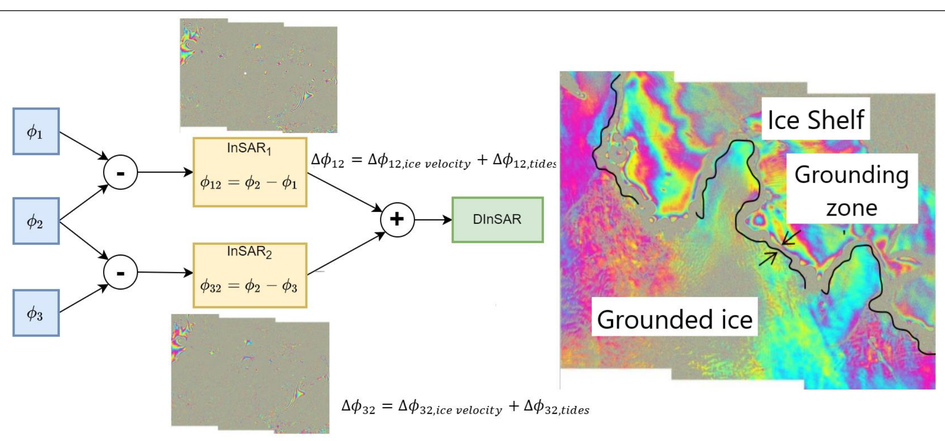

Dataset

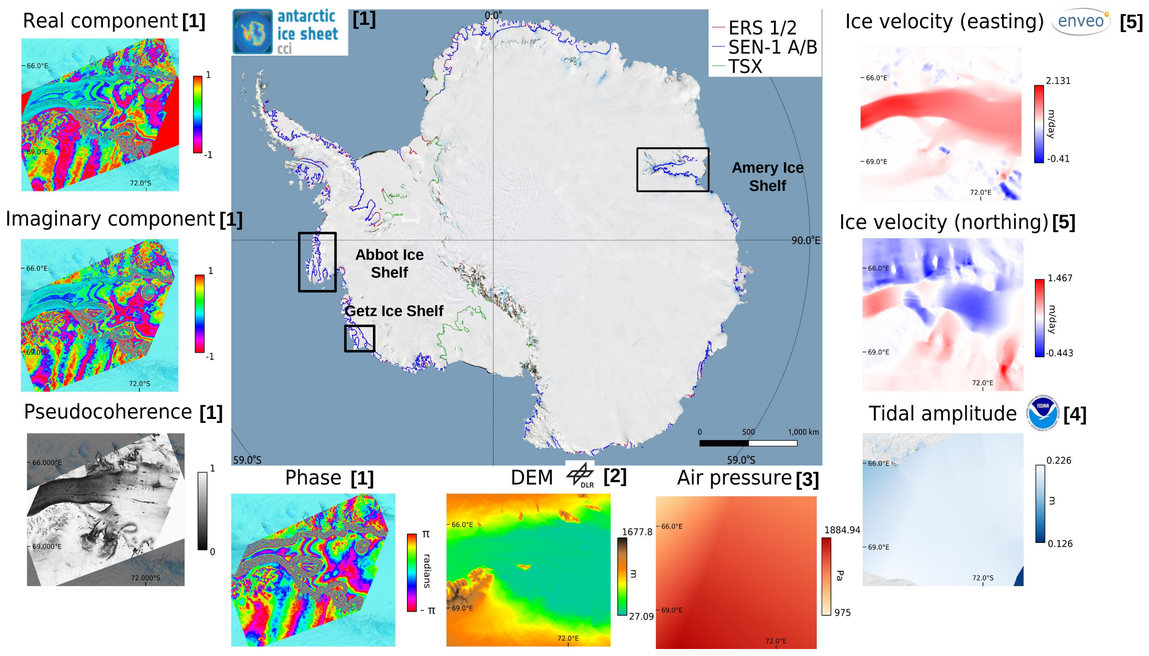

Satellite	Temporal extent [years]	Repeat cycle [days]	DInSAR interferograms
Sentinel 1 A/B	2014 – 2021	6,12	201
ERS 1/2	1992 – 1996	1,3	148
TerraSAR-X	2012 – 2018	11	129

The feature stacks were split into 4142 training tiles and 558 test tiles of dimension 256 x 256 pixels and 100 m pixel size

Processing chain

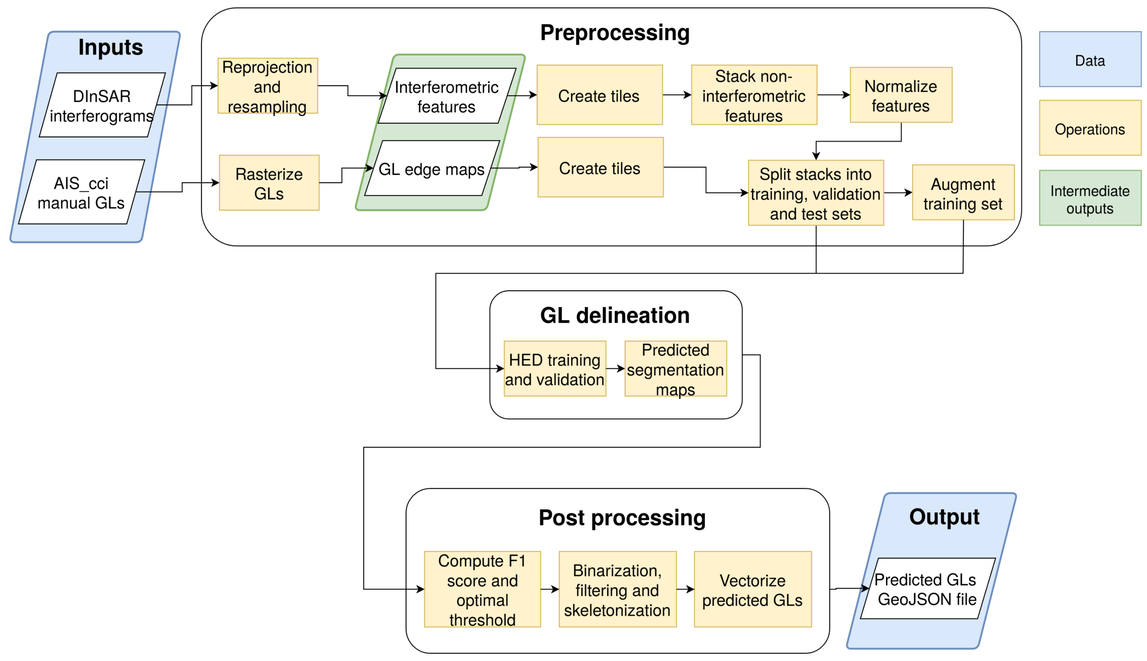

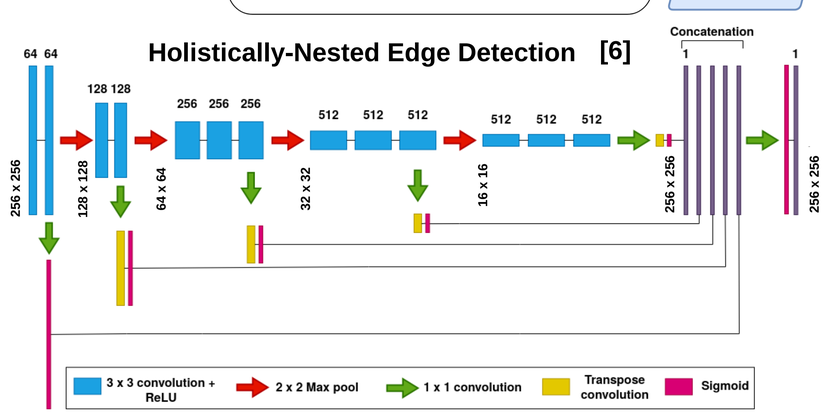

Metrics

The deviation between predictions and ground truth was computed using the metric for polygons and line segments (PoLiS) [7]

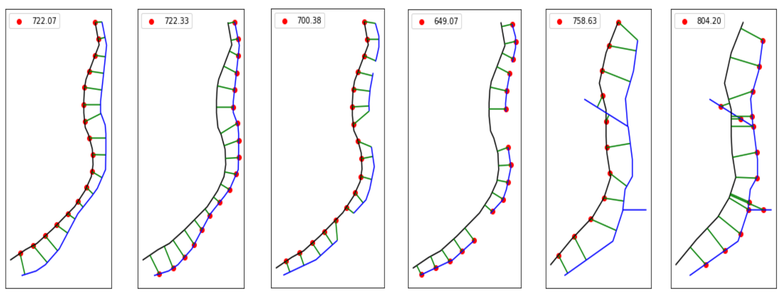

Results

- Real and imaginary interferogram components contribute more towards GLL detection than phase and pseudo coherence
- The network does not fully capture pinning points, small islands and sharp curves
- The network is robust against mislabeled samples

Features subset	Median deviation [m]	Median Absolute Deviation [m]
Phase & pseudo coherence + non-interferometric features	209.56	152.24
Phase & pseudo coherence	217.04	156.74
Real & imaginary components + non-interferometric features	**139.70**	**84.10**
Real & imaginary components	163.90	104.60

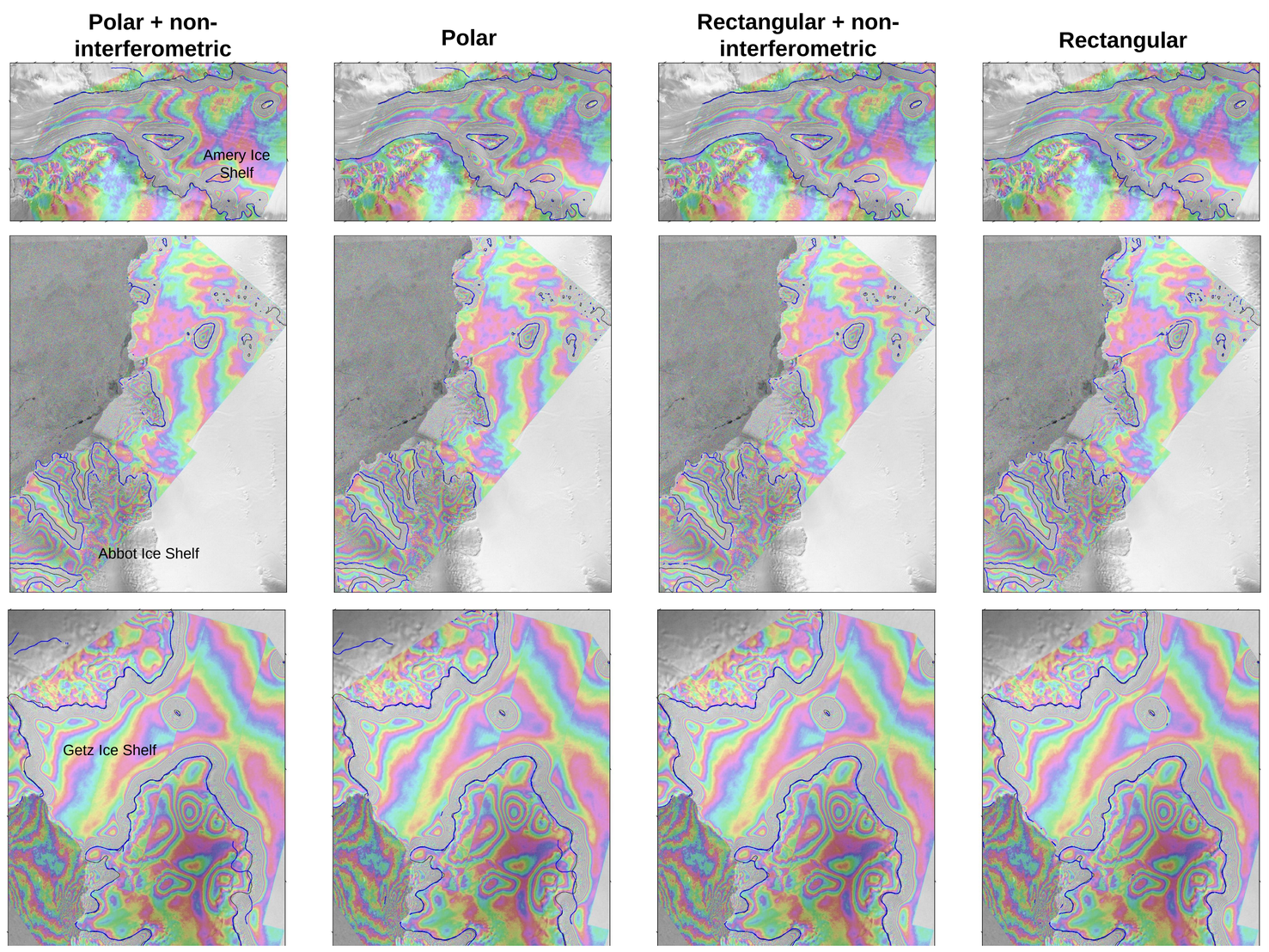

[1] A. Groh, Product User Guide (PUG) for the Antarctic Ice Sheet cci project of ESA' s Climate Change Initiative, version 1.0, 2021
[2] M. Huber, "TanDEM-X PolarDEM Product Description, prepared by German Remote Sensing Data Center (DFD) and Earth Observation Center", 2020
[3] E. Kalnay et al., "The NCEP/NCAR 40-year reanalysis project," *Bulletin of the American Meteorological Society*, 77(3), pp.437-472, 1996
[4] L. Padman et al., "Improving Antarctic tide models by assimilation of ICESat laser altimetry over ice shelves," *Geophysical Research Letters*, 35(22)
[5] T. Nagler et al., "The Sentinel-1 mission: New opportunities for ice sheet observations," *Remote Sensing*, vol. 7, no.7, pp.9371-9389, 2015
[6] S. Xie & Z. Tu, "Holistically-nested edge detection," in *Proceedings of the IEEE international conference on computer vision*, 2015, pp.1395-1403
[7] J. Avbelj et al., "A metric for polygon comparison and building extraction evaluation", *IEEE Geoscience and Remote Sensing Letters*, 2014 vol. 12, pp. 170-174

Contact: sindhu.ramanathtarekere@dlr.de

Deutsches Zentrum für Luft- und Raumfahrt